

CALICO: Confident Active Learning with Integrated Calibration

Lorenzo S. Querol¹, Hajime Nagahara^{1,2}, and Hideaki Hayashi¹

¹ Osaka University, Japan

{lorenzoquerol}@is.ids.osaka-u.ac.jp

{nagahara,hayashi}@ids.osaka-u.ac.jp

² Premium Research Institute for Human Metaverse Medicine (WPI-PRIME)

Abstract. The growing use of deep learning in safety-critical applications, such as medical imaging, has raised concerns about limited labeled data, where this demand is amplified as model complexity increases, posing hurdles for domain experts to annotate data. In response to this, active learning (AL) is used to efficiently train models with limited annotation costs. In the context of deep neural networks (DNNs), AL often uses confidence or probability outputs as a score for selecting the most informative samples. However, modern DNNs exhibit unreliable confidence outputs, making calibration essential. We propose an AL framework that self-calibrates the confidence used for sample selection during the training process, referred to as Confident Active Learning with Integrated Calibration (CALICO). CALICO incorporates the joint training of a classifier and an energy-based model, instead of the standard softmax-based classifier. This approach allows for simultaneous estimation of the input data distribution and the class probabilities during training, improving calibration without needing an additional labeled dataset. Experimental results showcase improved classification performance compared to a softmax-based classifier with fewer labeled samples. Furthermore, the calibration stability of the model is observed to depend on the prior class distribution of the data.

Keywords: Active learning · confidence calibration · energy-based models · medical imaging.

1 Introduction

The growing complexity of modern deep neural networks (DNNs) poses a challenge by demanding a substantial increase in labeled data needed to achieve state-of-the-art performance [8,27]. In real-world applications, obtaining labeled data is a logistically expensive process. This challenge is particularly profound in medical imaging, where images are complex and difficult to interpret, requiring the need for domain experts with clinical experience. This implies that a longer turnaround time is needed to finalize ground-truth annotations [3,27]. Given this time-consuming process, the ratio between labeled and unlabeled data samples

becomes aggravated. To tackle this issue, methods have been devised to optimize data efficiency in training models.

Active learning (AL), or human-in-the-loop learning [27], is one of the existing methods that aims to reduce the need for extensive labeled data. The intuition behind AL is to involve human knowledge in the learning process by iteratively selecting samples that are considered most informative by some heuristic function [20]. A subset of these samples is then given to a domain expert for annotation, thereby maximizing the performance of the model while concurrently minimizing the annotation costs.

In AL, the confidence outputs of a DNN are commonly used to select the most informative samples [24]. In classification using DNNs, confidence is typically defined by the maximum value of the class posterior probabilities (i.e., $\max_c p(c | x)$ for class c given an input sample x) calculated by the softmax function of the final layer. A lower confidence level indicates greater uncertainty in the model’s prediction, making it more beneficial to label such samples. Consequently, these low-confidence samples are prioritized as the most informative for selection.

However, the straightforward method of using a softmax-based classifier was revealed to produce uncalibrated outputs [9,10,18]. The problem arises from the characteristic of the cross-entropy loss function used in DNN training, where the loss decreases as the model’s confidence approaches one. This happens when the posterior probability for a particular class approaches one while diminishing to zero for other classes. As a result, the classifier may erroneously exhibit high confidence even for input samples that are difficult to classify. This phenomenon is commonly referred to as the over-confidence issue. In the context of an AL paradigm, uncalibrated confidence outputs could impede reliable decision-making during the selection of informative samples. Consequently, this may lead to poor performance of the learned model on unseen data.

Hence, a concept called *confidence calibration* in neural networks becomes a crucial aspect of developing modern intelligent systems. Confidence calibration is defined as the reflection of a model’s accuracy with its predictive confidence [10,16]. For instance, in scenarios where a classifier provides 100 predictions, each with 95% confidence, it is statistically expected that 95 of those predictions should be correct. In general, the calibration of neural networks is performed in a post-hoc manner, which calibrates the confidence output of the model after training. A common method for this is temperature scaling, which modifies the softmax function in the final layer by incorporating a temperature parameter, thereby calibrating the confidence output. However, post-hoc methods typically require a separate labeled dataset, inefficient in the context of AL as it consumes the already limited labeled data.

To calibrate the confidence output during the AL loop without relying on validation samples, our key idea involves leveraging the distribution of unlabeled training data. This is achieved through the simultaneous learning of a classifier and generative model. Fig. 1 outlines the advantages of this joint learning approach. Training a classifier in isolation often leads to inaccurately high posterior probability near the decision boundary. However, by concurrently estimating the

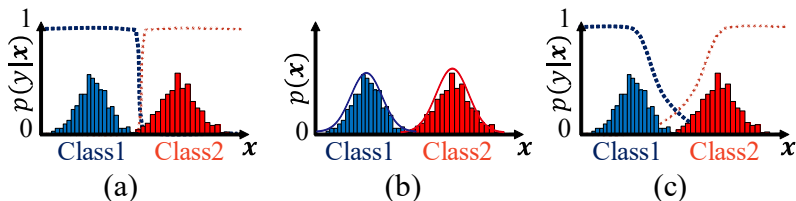


Fig. 1. Joint learning of a classifier and generative model and its advantage. (a) Training solely a classifier can lead to inaccurately high posterior probability near the class decision boundary. (b) Estimating the input distribution using a generative model allows us to account for the frequency of data occurrences. (c) Joint learning of the classifier and generative model helps to calibrate the confidence scores.

input data distribution with a generative model, the classifier is trained to account for the frequency of data occurrences. This approach naturally lowers the posterior probabilities for ambiguous data points near the decision boundary, leading to an inherent self-calibration of confidence levels.

We propose an AL framework designed to self-calibrate confidence during the training process. The method, called CALICO (Confident Active Learning with Integrated CalibratiOn), involves the joint training of a neural network-based classifier with an energy-based model (EBM) [14] in a semi-supervised manner. This joint training enhances the model’s understanding of the input data distribution, thereby calibrating the confidence outputs. The key idea is to use these calibrated confidence outputs as input for a query strategy, specifically using the least confidence strategy. This approach enhances decision reliability in selecting samples for annotation, with the overall goal of minimizing model miscalibration and improving accuracy with a minimal number of samples.

The contributions of this paper are as follows:

1. We propose an AL framework termed CALICO, which is designed to self-calibrate confidence during the training process. Our method involves joint training of a classifier and EBM to achieve calibration of confidence without separate validation samples, utilizing the calibrated confidence outputs to select the most informative samples.
2. We demonstrate that the self-calibration approach, which involves simultaneous learning of a classifier and a generative model, is effective for AL in terms of improving accuracy and decreasing calibration error using fewer labeled data than straightforward baseline methods.
3. We revealed the potential of class distribution balancing to enhance CALICO’s performance on datasets with class imbalance.

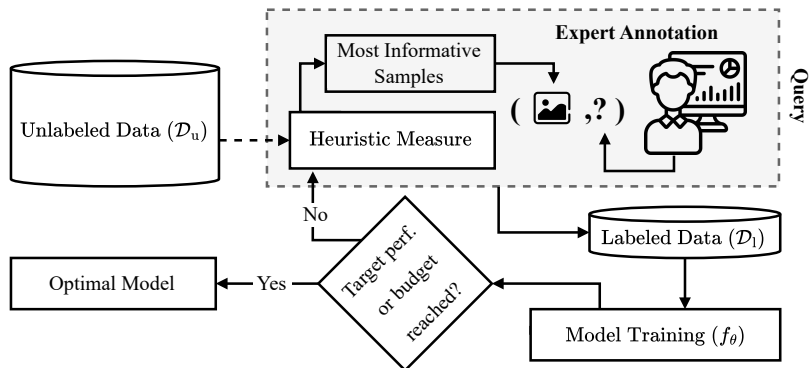


Fig. 2. An overview of the typical active learning (AL) cycle.

2 Background & Related Works

2.1 Active Learning

According to [20], allowing a learnable algorithm to select the data from which it learns can lead to more effective learning. In other words, AL seeks to maximize neural network performance with a smaller selection of data. As shown in Fig. 2, a typical AL scenario involves an *active learner* (model) continuously seeking new samples from a large pool of unlabeled data and inquiring the *oracle* (domain expert) for ground-truth annotations. The goal is to achieve a specific target performance, such as accuracy, while minimizing labeling costs. AL has been widely utilized in traditional machine learning tasks [20,6,13], but with the emerging use of DL achieving superior results in various tasks [24,8] comes with increasing dependence on the amount of labeled data gathered. Acquiring labeled data in task-specific or real-world problems is laborious and time-consuming, thus methods such as AL have become more relevant with its use in combination with DL, hence commonly referred to as deep AL [33].

Sample acquisition can be categorized into three main frameworks: membership query synthesis, stream-based sampling, and pool-based sampling. In real-world scenarios, it is common to acquire a large batch of unlabeled data at once, prompting the use of pool-based sampling [20]. The pool-based sampling framework assumes that there is a limited amount of labeled data and a more extensive pool of unlabeled data. To guide the active learner in selecting which data points to request labels for, samples are selected greedily via a *query strategy* [24]. The labels for the query are obtained by inquiring the oracle, and the data pools are consequently updated. The model is then retrained iteratively until a certain metric reaches a target value or the unlabeled data pool is exhausted. Various common query strategies, such as maximum entropy, margin, least confidence, and mean standard deviation-based approaches, have been established in AL. Moreover, the rise of frameworks like generative adver-

sarial networks and Bayesian deep learning [7,23] have also contributed to the development of enhanced query strategies in this field.

Despite extensive research on query strategies in AL, extending these methods to DL remains challenging, especially due to model uncertainty and inadequate labeled data [33]. The often utilized softmax response for deriving the class probability in DNNs exhibits overconfidence [25], posing possible difficulties in evaluating unlabeled data. This observation has attracted research attention towards deep Bayesian AL [7,8,23]. Furthermore, recent advances in uncertainty quantification have received interest for its use in AL paradigms [1,12]. However, these strategies frequently result in increased computation time for model training and inference, and may require altering the model architecture itself. To solve the dilemma of limited labeled data in deep learning, an approach involves reducing the issue by merging semi-supervised learning with AL [21]. This strategy uses unlabeled data to gather more information about the data distribution and improves the model’s overall performance.

2.2 Energy-Based Models

An EBM is a type of generative model that directly models a negative log-probability, which is also known as the energy function. The model’s probability density function is derived by normalizing the energy function, expressed as $p_{\theta}(\mathbf{x}) = \exp(-E_{\theta}(\mathbf{x}))/Z_{\theta}$. In this formulation, E_{θ} is the energy function parameterized by θ , and Z_{θ} is the normalizing constant, computed as $Z_{\theta} = \int_{\mathbf{x}} \exp(-E_{\theta}(\mathbf{x}))d\mathbf{x}$. A key challenge in working with EBMs is that this integral for the normalizing term is typically intractable. To estimate it, advanced sampling techniques are often employed, such as using Markov chain Monte Carlo (MCMC) and stochastic gradient Langevin dynamics (SGLD) [26].

EBMs are utilized in a vast range of applications such as image generation [5], texture generation [28], and text generation [4,2]. EBMs have also applied in the context of dropout and pruning within NNs [19]. Additionally, EBMs can be utilized for the complex problem of continuous inverse optimal control [29]. There have been several approaches to simultaneously training an EBM and a classifier [31,15,32,11], revealing the effectiveness of EBMs for semi-supervised learning, outlier detection, and confidence calibration.

2.3 Confidence Calibration

Formally, considering a dataset with input x and outcome $y \in \{1, \dots, K\}$, a neural network is considered *perfectly calibrated* if:

$$p(Y = y \mid \hat{c} = c) = c, \quad \forall c \in [0, 1] \quad (1)$$

Here, \hat{c} represents the probability of a predicted label Y , and y is the ground-truth label. Model calibration is frequently depicted using reliability diagrams [10], where the expected accuracy is plotted as a function of confidence. Perfect

Algorithm 1 CALICO: Confident Active Learning with Integrated Calibration

-
- 1: **Input:** Labeled dataset \mathcal{D}_l , Unlabeled pool \mathcal{D}_u , Query Size Q , Number of queries N_q , Query strategy α^{LC} , Oracle g
 - 2: **Initialize:** Model f_θ
 - 3: **while** $1 \leq i \leq N_q$ **do**
 - 4: **Train:** Train f_θ over $\mathcal{D}_l \cup \mathcal{D}_u$
 - 5: $\mathcal{D}_q \leftarrow \alpha^{\text{LC}}(\mathcal{D}_u, Q, f_\theta)$
 - 6: $\mathcal{D}_l \leftarrow \mathcal{D}_l \cup g(\mathcal{D}_q)$
 - 7: $\mathcal{D}_u \leftarrow \mathcal{D}_u \setminus \mathcal{D}_q$
 - 8: **Evaluate:** Compute performance of f_θ on a valid. set
 - 9: **end while**
 - 10: **Output:** Trained model f_θ
-

calibration is plotted similarly as an identity function, and any deviation from the diagonal signifies miscalibration.

Literature reveals that the utilization of modern neural networks with increasing complexity often results in poor calibration [10,16]. Therefore, various methods have been proposed to calibrate confidence. The calibration methods can be classified into two categories: post-hoc calibration and train-time calibration. Post-hoc calibration is one performed after training. It has been a primal approach, and many methods have been proposed [10]. Among such methods, temperature scaling [10] is considered simple and effective. It uses a softmax function with temperature instead of the usual softmax in the final layer of the NN and tunes the temperature parameter to optimize the negative likelihood. In contrast, train-time calibration is performed during training, which involves simultaneous learning with generative models [9,11] and the use of soft labels [22]. The main difference between post-hoc and train-time methods is whether the validation data is used to calibrate the confidence.

3 CALICO: Confident Active Learning with Integrated Calibration

The proposed CALICO achieves efficient learning by utilizing calibrated confidence when selecting samples to be labeled. Confidence calibration is performed during the AL process by simultaneously estimating the input data distribution with an EBM and the class posterior probabilities with a classifier.

3.1 Algorithm of CALICO

The details of CALICO are described in Algorithm 1. Suppose that we have a limited amount of labeled data $\mathcal{D}_l = \{(\mathbf{x}_i, y_i)\}_{i=1}^M$, and a more extensive pool of unlabeled data $\mathcal{D}_u = \{\mathbf{x}_i\}_{i=1}^N$, where $M < N$, and $y_i \in \{1, \dots, K\}$ is the class label of input \mathbf{x}_i . The model f_θ is trained over both \mathcal{D}_l and \mathcal{D}_u . The use of unlabeled data is enabled by simultaneous learning with an EBM, and this

point differs from traditional AL processes. The query \mathcal{D}_q is a subset of \mathcal{D}_u and is selected based on a predefined query size Q and query strategy α^{LC} , which is detailed in the next subsection. The labels for \mathcal{D}_q are obtained by inquiring with the oracle g , and \mathcal{D}_q with the obtained labels is denoted as $g(\mathcal{D}_q)$. Subsequently, both data pools are updated accordingly where $\mathcal{D}_l \leftarrow \mathcal{D}_l \cup g(\mathcal{D}_q)$, and $\mathcal{D}_u \leftarrow \mathcal{D}_u \setminus \mathcal{D}_q$. The model f_θ is then retrained iteratively until a certain metric reaches a target value or the unlabeled data pool \mathcal{D}_u is exhausted.

3.2 Query Strategy

We utilize a least confidence strategy [24]. The least confidence query strategy is designed to acquire samples with the smallest probability among the maximum activations. Given an unlabeled data pool \mathcal{D}_u , trained model f_θ , and the query size Q , the strategy α^{LC} is defined as follows:

1. Compute the posterior probability $p_\theta(y | \mathbf{x})$ for all $x \in \mathcal{D}_u$ based on (2).
2. Obtain the corresponding confidence $\max_y(p_\theta(y|\mathbf{x}))$.
3. Sort the samples in \mathcal{D}_u in ascending order with respect to the confidence.
4. The strategy α^{LC} returns the top Q samples.

Based on this strategy, a set of samples is selected from the unlabeled data pool to query the oracle for annotation.

3.3 Joint Learning of a Classifier and an Energy-based Model

Among various methods proposed for joint learning of a classifier and an EBM [9,31,32,11], we construct our model f_θ with reference to the structure of JEM [9]. The model consists of a single neural network with a multi-head output for classification and EBM. Given an input $\mathbf{x} \in \mathbb{R}^D$, the model first outputs a real-valued K -dimensional vector, i.e., $f_\theta : \mathbb{R}^D \rightarrow \mathbb{R}^K$. The vector is then converted into the class posterior probability in the classification head and the probability density of input data in the EBM head. In the classification head, the posterior probability of class $y \in \{1, \dots, K\}$ is calculated through the standard softmax transfer function, as defined below:

$$p_\theta(y | \mathbf{x}) = \frac{\exp(f_\theta(\mathbf{x})[y])}{\sum_{y'=1}^K \exp(f_\theta(\mathbf{x})[y'])}, \quad (2)$$

where $f_\theta(\mathbf{x})[y]$ indicates the logit corresponding to y -th class. In the EBM head, the probability density $p(\mathbf{x})$ is computed as follows:

$$p_\theta(\mathbf{x}) = \frac{\sum_{y=1}^K \exp(f_\theta(\mathbf{x})[y])}{Z(\theta)}, \quad (3)$$

where $Z(\theta) = \int_{\mathbf{x}} \sum_{y=1}^K \exp(f_\theta(\mathbf{x})[y])d\mathbf{x}$ is the normalizing constant, otherwise known as the partition function.

In the training of the hybrid model, we minimize the following loss function over the union of labeled and unlabeled datasets $\{(\mathbf{x}_n, y_n)\}_{i=1}^M \cup \{\mathbf{x}_i\}_{i=M+1}^{M+N}$.

$$\mathcal{L} = - \sum_{i=1}^M \log p(y_i | \mathbf{x}_i) - \sum_{i=1}^{M+N} \log p(\mathbf{x}_i), \quad (4)$$

where the first term on the right-hand side corresponds to cross-entropy and is optimized via conventional stochastic gradient descent. The second term is the negative log-likelihood for the EBM optimization whose gradient can be computed using stochastic gradient Langevin dynamics (SGLD).

As a distinction from the original JEM training algorithm, we incorporate techniques from recent EBM studies to stabilize and accelerate training. First, we adopt the informative initialization [31], which uses samples from a Gaussian mixture distribution estimated from the training dataset instead of random noise samples for initializing the SGLD chain. Second, we employ Proximal-YOPO-SGLD [31], which freezes the gradient with respect to the second and subsequent layers during the sample updates. Third, we exclude data augmentation from the maximum likelihood estimation pipeline to alleviate the adverse effects of data augmentation on image generation quality [32].

4 Experiments

4.1 Experimental conditions

To verify the validity of CALICO, we conducted experiments using medical image datasets. We used five benchmark medical imaging datasets found in the MedMNIST collection [30], namely Blood, Derma, OrganS, OrganC, and Pneumonia. These medical imaging datasets consist of preprocessed 28×28 two-dimensional images, accompanied by their corresponding class labels. The classification tasks within these datasets range from binary to multi-class, serving as benchmarks for foundational models in the medical imaging domain.

The model closely followed the setup of [31]. However, we changed the ReLU activation function used by the Wide-ResNet architecture to a Swish activation function for the added stability observed by [5]. As the computational training time of JEM++ is also relatively long, we limited the number of queries for all datasets (more details in Appendix).

We evaluated the results based on classification accuracy and calibration errors. Miscalibration can be condensed into a convenient scalar metric, often quantified as the expected calibration error (ECE) [17]. This metric discretizes probability intervals into a fixed number of bins and the calibration error is calculated as the difference between the fraction of correct predictions (accuracy), and the mean of the probabilities in the bin (confidence). ECE computes a weighted average of this error across bins:

$$\text{ECE} = \sum_{m=1}^{M_{\text{bin}}} \frac{|\mathcal{B}_m|}{N_{\text{data}}} | \text{acc}(\mathcal{B}_m) - \text{conf}(\mathcal{B}_m) | \quad (5)$$

Table 1. Performance Comparison of Test Accuracy (\uparrow) and ECE (\downarrow) Values

Dataset	Criterion (%)	Baseline	Active	CALICO
Blood	Best ACC / ECE	95.82 / 0.95	95.47 / 1.73	96.43 / 0.54
	Final ACC / ECE	-	95.44 / 1.87	96.00 / 0.56
Derma	Best ACC / ECE	74.02 / 3.50	74.87 / 1.82	76.37 / 1.89
	Final ACC / ECE	-	74.56 / 1.82	75.66 / 1.89
OrganS	Best ACC / ECE	78.54 / 6.75	78.55 / 10.04	79.90 / 7.00
	Final ACC / ECE	-	78.55 / 10.04	79.90 / 7.00
OrganC	Best ACC / ECE	89.54 / 5.31	89.79 / 4.17	90.34 / 3.03
	Final ACC / ECE	-	88.58 / 5.76	90.26 / 3.03
Pneumonia	Best ACC / ECE	87.66 / 12.33	89.26 / 9.73	89.26 / 9.82
	Final ACC / ECE	-	87.66 / 12.33	86.22 / 11.88

where \mathcal{B}_m represents the subset of samples whose predicted confidence levels lie within the interval $I_m = (\frac{m-1}{M_{\text{bin}}}, \frac{m}{M_{\text{bin}}}]$, N_{data} is the total number of data points, and $\text{acc}(\mathcal{B}_m)$ and $\text{conf}(\mathcal{B}_m)$ denote the accuracy and confidence of \mathcal{B}_m , respectively. For this study, we utilize ECE as the primary metric for measuring calibration, as well as reliability diagrams for visualization.

We establish the baseline reference by maximizing only the $\log p(y|x)$ objective through the utilization of the entire dataset, with a softmax-based classifier (named **Baseline**), involving the evaluation of calibration error using the probability outputs from the softmax activation function and calculating the ECE. We also used a softmax-based classifier paired with an AL framework using the least confidence query strategy (named **Active**) as an additional baseline reference.

4.2 Performance Comparison

Table 1 shows that CALICO consistently outperformed the baseline accuracy across all evaluated datasets. In parallel with the accuracy improvements, CALICO also showed reduced ECEs, indicating its effectiveness in minimizing miscalibration. We observed that using a softmax-based classifier within an AL paradigm, as opposed to straightforward training methods, resulted in better calibration. However, CALICO demonstrated a more substantial increase in performance when compared to the baseline, suggesting its effectiveness in improving the classifier’s performance in an AL paradigm. While CALICO generally achieved lower ECE values across most datasets, the use of a softmax-based classifier in an AL paradigm demonstrated comparable efficacy to CALICO in some cases, such as Derma and OrganS.

4.3 Confidence Calibration

The final reliability diagrams are depicted in Fig. 3. A perfectly calibrated model would align with the red-diagonal dashed line, effectively creating an identity

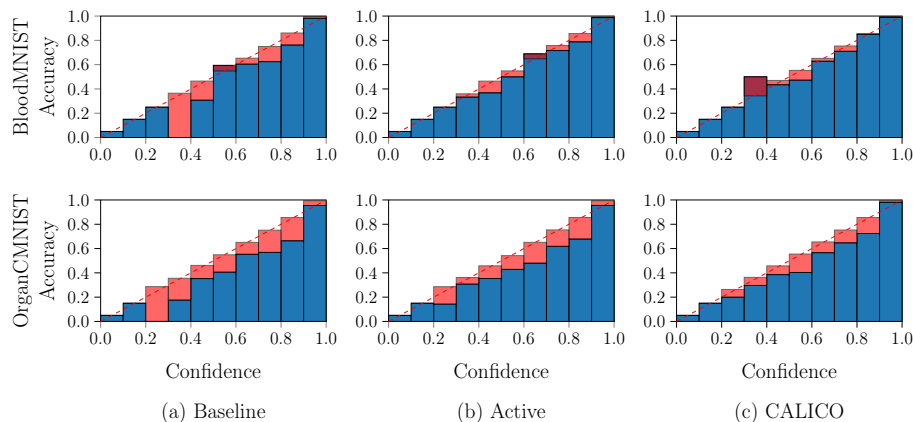


Fig. 3. The final reliability diagrams for the baseline, active, and CALICO. In comparison, CALICO demonstrated a substantial improvement in calibration across confidence intervals when compared to the other evaluated methods that used softmax-based classifiers.

function between the y-axis (accuracy) and the x-axis (confidence intervals). Any deviation above or below this diagonal indicates underconfidence or overconfidence, respectively, representing miscalibration. It is prominent that there is a marginal difference in the improvement of overconfident intervals between using softmax-based classifiers and CALICO, emphasizing the effectiveness of calibrated confidence outputs for iterative training in an AL paradigm.

4.4 Learning Curve Analysis

Learning curves play a crucial role in assessing how well a model performs in an AL paradigm, particularly by observing a specific metric with respect to the number of labeled samples. In this study, the ECE is of certain importance. Similar to the commonly used accuracy, the goal is to determine whether miscalibration can be minimized with significantly fewer labeled samples through the utilization of JEMs. As illustrated in Fig. 4, the overall calibration trend using CALICO is observed to be lower than that of the softmax-based classifiers. Additionally, it is noteworthy that a lower or comparable ECE can be achieved with fewer samples in comparison to the baseline reference.

4.5 Performance Comparison of Test Accuracy and ECE Values with an Equal Class Distribution

We explored the impact of class distribution balancing on CALICO’s performance. While many confidence calibration studies emphasize calibration error within balanced class distributions, achieving such balance is not guaranteed in AL due to sampling methods’ greedy nature. Calibration learning curves (Fig.

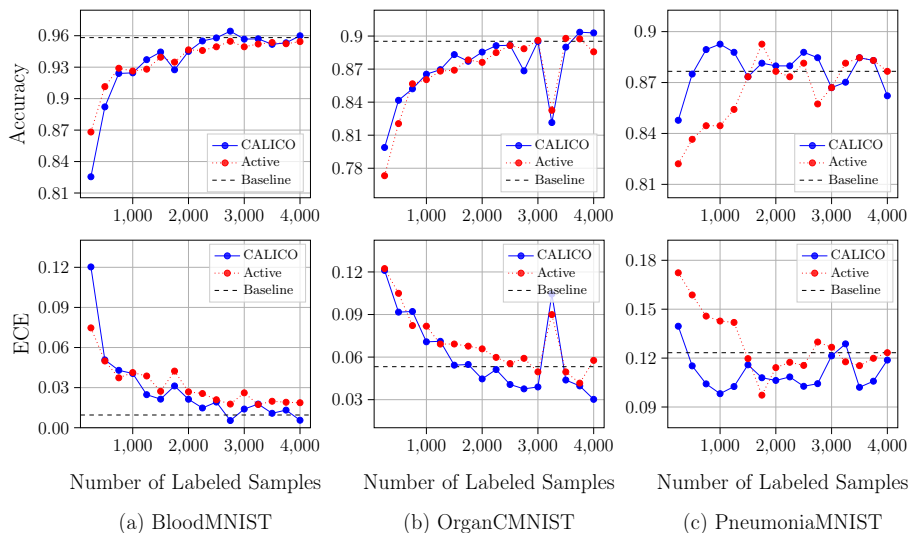


Fig. 4. The test accuracy (top) and ECE (bottom) values plotted against the number of labeled samples per AL iteration. It can be observed that a lower or comparable ECE value can be achieved with a lesser number of labeled samples.

4) exhibited instability, possibly due to overconfidence from uncertainty-based sampling. Additionally, inherent dataset class imbalances can lead to querying uninformative samples, creating a mode collapse problem and miscalibration. To simulate literature setups, CALICO’s performance was evaluated with an equal class distribution (named **Equal**), enforcing limits based on the dataset’s least represented class. Varying labels per class allowed for sufficient iterations to analyze learning curves. Experimental setup details are provided in Table 3 of Appendix.

We observed instances where having an equal class distribution yielded better calibration or more stable learning curves across the evaluated datasets, such as the results on the PneumoniaMNIST dataset. However, Table 2 also highlights instances where equal class distribution did not result in better calibration compared to the original CALICO. One possible explanation for this disparity is the nature of the datasets; PneumoniaMNIST is an imbalanced binary dataset, while others are relatively balanced multi-class datasets, and balancing the class ratio in sample selection facilitated effective learning of information from the minority class. These findings imply the potential of class distribution balancing to enhance CALICO’s performance on imbalanced datasets.

5 Conclusion

We proposed an AL method called CALICO, which aimed to use the calibrated confidence outputs as the input for a query strategy in an AL paradigm. CAL-

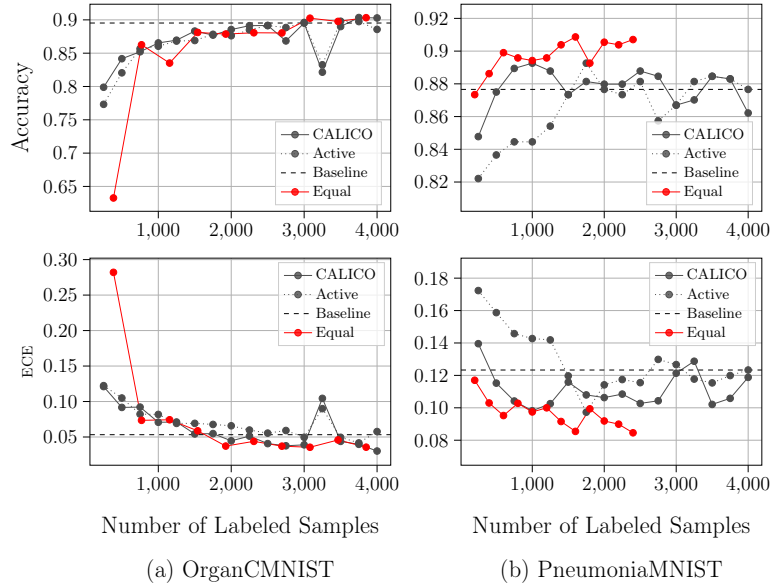


Fig. 5. The test accuracy (top) and ECE (bottom) values of CALICO with an equal class distribution. Note that the *Equal* method was designed to strictly enforce an equal distribution by setting a limit based on the dataset’s class label with the fewest samples. Additionally, the number of labels per class varied per dataset to allow for an adequate number of iterations to properly analyze the learning curve.

ICO incorporates the joint training of a classifier and an EBM, allowing self-calibration of confidence used for sample selection in AL. Experimental results demonstrated that CALICO outperformed the baseline accuracy and achieved a lower ECE with less labeled data, compared to a softmax-based classifier.

One of the limitations of this study is scalability because training an EBM on high-resolution images requires considerable hyperparameter tuning, and CALICO was only evaluated on small-resolution images. Future research could explore the applications of CALICO with other AL methods, harnessing the power of Bayesian approaches for better uncertainty quantification. Additionally, further evaluation of larger datasets in other domains can broaden the scope and applicability of this research domain.

Appendix

Experimental Setup To ensure consistency across all experiments, the computational runtime constraints necessitated limiting each dataset to 4000 labeled samples, with a query size of 250 for each iteration, resulting in a total of 16 iterations. In the ablation study that focused on an equal class distribution, the experimental setup was detailed in Table 3. The number of labeled samples

Table 2. Min. and Final Test Accuracy (\uparrow) and ECE (\downarrow) Values in Comparison to an Equal Class Distribution

Dataset	Criterion (%)	Baseline	CALICO	Equal
Blood	Best ACC / ECE	95.82 / 0.95	96.43 / 0.54	96.25 / 0.89
	Final ACC / ECE	-	96.00 / 0.56	96.05 / 0.89
OrganS	Best ACC / ECE	78.54 / 6.75	79.90 / 7.00	78.98 / 10.49
	Final ACC / ECE	-	79.90 / 7.00	78.07 / 10.49
OrganC	Best ACC / ECE	89.54 / 5.31	90.34 / 3.03	90.25 / 3.56
	Final ACC / ECE	-	90.26 / 3.03	90.32 / 3.57
Pneumonia	Best ACC / ECE	87.66 / 12.33	89.26 / 9.82	90.87 / 8.46
	Final ACC / ECE	-	86.22 / 11.88	90.71 / 8.46

Table 3. Experimental Setup for Equal Class Distribution

Dataset	Lowest Count (Class)	Limit	Labels per Class
Blood	849 (lymphocyte)	4,000	50
OrganS	614 (femur-right)	3,850	35
OrganC	600 (heart)	3,850	35
Pneumonia	1,214 (normal)	2,400	100

per class for each iteration was determined by the class with the fewest samples to create enough iterations for analysis. The only exception to the ablation study was the DermaMNIST dataset, where the class with the lowest number of samples was 89. It was decided not to include this dataset in the ablation study.

Hyperparameter Settings All datasets, except for PneumoniaMNIST, adapted the default hyperparameters from the original literature of JEM++ [31]. This included using an SGD optimizer with a learning rate of 0.1. However, for PneumoniaMNIST, an Adam optimizer with a learning rate of 0.0001 was utilized, as it exhibited a more stable calibration performance.

Acknowledgments. This work was supported by JSPS KAKENHI Grant Number JP24K03010 and the World Premier International Research Center Initiative (WPI), MEXT, Japan.

References

1. Abdar, M., Pourpanah, F., Hussain, S., Rezazadegan, D., Liu, L., Ghavamzadeh, M., Fieguth, P., Cao, X., Khosravi, A., Acharya, U.R., et al.: A review of uncertainty quantification in deep learning: Techniques, applications and challenges. *Information fusion* **76**, 243–297 (2021)
2. Bakhtin, A., Deng, Y., Gross, S., Ott, M., Ranzato, M., Szlam, A.: Residual energy-based models for text. *Journal of Machine Learning Research* **22**(40), 1–41 (2021)

3. Budd, S., Robinson, E.C., Kainz, B.: A survey on active learning and human-in-the-loop deep learning for medical image analysis. *Medical Image Analysis* **71**, 102062 (2021)
4. Deng, Y., Bakhtin, A., Ott, M., Szlam, A., Ranzato, M.: Residual energy-based models for text generation. In: *Proceedings of the International Conference on Learning Representations* (2020)
5. Du, Y., Mordatch, I.: Implicit generation and modeling with energy based models. In: *Proceedings of the Annual Conference on Neural Information Processing Systems*. vol. 32 (2019)
6. Fu, Y., Zhu, X., Li, B.: A survey on instance selection for active learning. *Knowledge and Information Systems* **35**, 249–283 (2013)
7. Gal, Y., Ghahramani, Z.: Bayesian convolutional neural networks with Bernoulli approximate variational inference. *arXiv preprint arXiv:1506.02158* (2015)
8. Gal, Y., Islam, R., Ghahramani, Z.: Deep Bayesian active learning with image data. In: *Proceedings of the International Conference on Machine Learning*. pp. 1183–1192. PMLR (2017)
9. Grathwohl, W., Wang, K.C., Jacobsen, J.H., Duvenaud, D., Norouzi, M., Swersky, K.: Your classifier is secretly an energy based model and you should treat it like one. In: *Proceedings of the International Conference on Learning Representations* (2020)
10. Guo, C., Pleiss, G., Sun, Y., Weinberger, K.Q.: On calibration of modern neural networks. In: *Proceedings of the International Conference on Machine Learning*. pp. 1321–1330 (2017)
11. Hayashi, H.: A hybrid of generative and discriminative models based on the Gaussian-coupled softmax layer. *IEEE Transactions on Neural Networks and Learning Systems (Early Access)* (2024)
12. Hein, A., Röhr, S., Grobel, T., Leng, M., Hafez, N., Knopp, M., Klenk, C., Heim, D., Hayden, O., Diepold, K.: A comparison of uncertainty quantification methods for active learning in image classification. In: *Proceedings of the International Joint Conference on Neural Networks*. pp. 1–8 (2022)
13. Kumar, P., Gupta, A.: Active learning query strategies for classification, regression, and clustering: a survey. *Journal of Computer Science and Technology* **35**, 913–945 (2020)
14. LeCun, Y., Chopra, S., Hadsell, R., Ranzato, M., Huang, F.: A tutorial on energy-based learning. *Predicting structured data* **1** (2006)
15. Liu, X., Staudt, D., Lin, C.T., Zach, C.: Effortless training of joint energy-based models with sliced score matching. In: *Proceedings of the International Conference on Pattern Recognition*. pp. 2643–2649 (2022)
16. Minderer, M., Djolonga, J., Romijnders, R., Hubis, F., Zhai, X., Houlsby, N., Tran, D., Lucic, M.: Revisiting the calibration of modern neural networks. In: *Proceedings of the Advances in Neural Information Processing Systems*. vol. 34, pp. 15682–15694 (2021)
17. Naeini, M.P., Cooper, G., Hauskrecht, M.: Obtaining well calibrated probabilities using Bayesian binning. In: *Proceedings of the AAAI Conference on Artificial Intelligence*. vol. 29 (2015)
18. Ren, P., Xiao, Y., Chang, X., Huang, P.Y., Li, Z., Gupta, B.B., Chen, X., Wang, X.: A survey of deep active learning. *ACM Computing Surveys* **54**, 1–40 (2021)
19. Salehinejad, H., Valaee, S.: EDropout: Energy-based dropout and pruning of deep neural networks. *IEEE Transactions on Neural Networks and Learning Systems* **33**(10), 5279–5292 (2022)

20. Settles, B.: Active learning literature survey. Computer Sciences Technical Report 1648, University of Wisconsin–Madison (2009)
21. Siméoni, O., Budnik, M., Avrithis, Y., Gravier, G.: Rethinking deep active learning: Using unlabeled data at model training. In: Proceedings of the International Conference on Pattern Recognition. pp. 1220–1227 (2021)
22. Thulasidasan, S., Chennupati, G., Bilmes, J.A., Bhattacharya, T., Michalak, S.: On mixup training: Improved calibration and predictive uncertainty for deep neural networks. Proceedings of the Annual Conference on Neural Information Processing Systems **32** (2019)
23. Tran, T., Do, T.T., Reid, I., Carneiro, G.: Bayesian generative active deep learning. In: Proceedings of the International Conference on Machine Learning. pp. 6295–6304 (2019)
24. Wang, D., Shang, Y.: A new active labeling method for deep learning. In: Proceedings of the International Joint Conference on Neural Networks. pp. 112–119. IEEE (2014)
25. Wang, K., Zhang, D., Li, Y., Zhang, R., Lin, L.: Cost-effective active learning for deep image classification. IEEE Transactions on Circuits and Systems for Video Technology **27**(12), 2591–2600 (2016)
26. Welling, M., Teh, Y.W.: Bayesian learning via stochastic gradient Langevin dynamics. In: Proceedings of the International Conference on Machine Learning. pp. 681–688 (2011)
27. Wu, X., Xiao, L., Sun, Y., Zhang, J., Ma, T., He, L.: A survey of human-in-the-loop for machine learning. Future Generation Computer Systems **135**, 364–381 (2022)
28. Xie, J., Lu, Y., Gao, R., Wu, Y.N.: Cooperative learning of energy-based model and latent variable model via MCMC teaching. In: Proceedings of the Annual AAAI Conference on Artificial Intelligence. vol. 32 (2018)
29. Xu, Y., Xie, J., Zhao, T., Baker, C., Zhao, Y., Wu, Y.N.: Energy-based continuous inverse optimal control. IEEE Transactions on Neural Networks and Learning Systems pp. 1–15 (2022)
30. Yang, J., Shi, R., Wei, D., Liu, Z., Zhao, L., Ke, B., Pfister, H., Ni, B.: MedM-NIST v2-A large-scale lightweight benchmark for 2D and 3D biomedical image classification. Scientific Data **10**(1), 41 (2023)
31. Yang, X., Ji, S.: JEM++: Improved techniques for training JEM. In: Proceedings of the IEEE/CVF International Conference on Computer Vision. pp. 6494–6503 (2021)
32. Yang, X., Su, Q., Ji, S.: Towards bridging the performance gaps of joint energy-based models. In: Proceedings of the IEEE/CVF Conference on Computer Vision and Pattern Recognition. pp. 15732–15741 (2023)
33. Zhang, Z., Strubell, E., Hovy, E.: A survey of active learning for natural language processing. In: Proceedings of the Conference on Empirical Methods in Natural Language Processing. pp. 6166–6190. Association for Computational Linguistics (2022)